Elastic and Inelastic Proton Scattering from Even Isotopes of Cd, Sn, and Te†

W. MAKOFSKE, W. SAVIN, H. OGATA,* AND T. H. KRUSE
Department of Physics, Rutgers, The State University, New Brunswick, New Jersey
(Received 18 April 1968)

Protons of 16-MeV energy were scattered from isotopically enriched targets of ^{110,112,114,116}Cd, ^{112,116,118,120,122,124}Sn, and ^{126,128,130}Te. Differential cross sections were measured for scattering to the 0^+ ground state and the first 2^+ and 3^- collective states. As the mass number A increases, the elastic angular distributions shift towards smaller angles and show increasing damping. The 2^+ and 3^- cross sections show a systematic decrease in magnitude with increasing A. Optical-model calculations were made by fixing the geometrical parameters for each set of isotopes and searching on V and W_D, the real and surface imaginary parts of the optical potential. The observed trends, systematically increasing with A, are consistent with an isospin dependence in the real and imaginary parts of the optical potential. The distorted-wave program DWUCK, assuming a collective vibrational model, was run using complex coupling and Coulomb excitation in order to extract deformation parameters β_l for all the 2^+ and 3^- states. These parameters indicate that the decrease in inelastic scattering with increasing A is associated with a decreasing collectivity for each set of isotopes. The values of β_l are in reasonable agreement with deformation parameters extracted by other methods.

I. INTRODUCTION

SYSTEMATIC studies of elastic and inelastic scattering of nucleons have yielded much information on nuclear structure and nuclear forces. Use of the optical model in fitting elastic scattering data has provided an approximate way of coping with the many-body problem. Distorted-wave theory, using a collective model description for the excitation of the one-phonon quadrupole and one-phonon octupole states in a variety of nuclei, has been successful in describing the inelastic angular distributions. Theoretical predictions are normalized to the experimental cross sections to extract values of β_l^2. These are usually in agreement with those found by Coulomb excitation and other types of measurements.

Because of recent interest in the "vibrational" region around $A=120$ due to quadrupole moment measurements,[1–4] and because the tin isotopes in this region are singly magic with a large range of $(N-Z)/A$, attention was focused on the A region 110–130.

Differential cross sections of elastically and inelastically scattered 16-MeV protons were measured in this study. The cross sections for the elastic scattering were fit in a systematic manner. Inelastic scattering to the one-phonon 2^+ and 3^- states was calculated with a distorted-wave program using the elastic optical parameters. Deformation parameters, β_2 and β_3, were extracted and comparisons were made with values obtained by other methods.

II. EXPERIMENTAL PROCEDURE

The Rutgers-Bell tandem Van de Graaff accelerator provided a 16-MeV beam of protons which were scattered from enriched targets of various isotopes. These targets were made by three different methods. Cadmium and a few tin targets were rolled to a thickness of 1–4 mg/cm^2. Thin cadmium, tin, and tellurium targets were made by evaporation onto a carbon-coated slide. These were typically 500–800 μg/cm^2 and contained sizable carbon and oxygen impurities. A few tin targets were also made by electroplating. Scattered protons were detected by lithium-drifted silicon semiconductor detectors of 2- and 3-mm depletion depth. In the latter part of the data collection a multiplexed system of two detectors 20° apart was utilized. The pulses were preamplified, amplified, converted, and stored in an on-line SDS 910 computer. The resolution of this system varied between 40 and 100 kV. Further details of the experimental arrangement are available in a previous work.[5]

The absolute normalizations of the cross sections were determined by a low-energy Rutherford angular distribution at the same target orientation as the high-energy data. On the basis of reproducibility of the absolute cross sections on different targets of the same isotope, the estimated error in the absolute normalizations is about 5%. Relative errors for the elastic scattering data points varied from 1–3% and were determined by the number of counts in the peak and reproducibility. Errors on the 2^+ and 3^- states were between 5–10% and were calculated from the peak areas, reproducibility, and background subtraction.

† Work supported in part by the National Science Foundation.
* On leave from Kyoto University, Japan.
[1] J. de Boer, R. G. Stokstad, G. D. Symons, and A. Winther, Phys. Rev. Letters **14**, 564 (1965).
[2] D. Eccleshall, M. J. L. Yates, and J. J. Simpson, in *Proceedings of the Symposium on Recent Progress in Nuclear Physics with Tandems, Heidelberg, 1966,* edited by W. Hering (Max Planck Institute for Nuclear Physics, Heidelberg, 1966).
[3] A. M. Kleinfeld, J. de Boer, Renata Covello-Moro, and H. P. Lie, Bull. Am. Phys. Soc. **12**, 564 (1967).
[4] P. H. Stelson, W. T. Milner, J. L. C. Ford, Jr., F. K. McGowan, and R. L. Robinson, Bull. Am. Phys. Soc. **10**, 429 (1965).
[5] P. Stoler, M. Slagowitz, W. Makofske, and T. H. Kruse, Phys. Rev. **155**, 1334 (1967).

III. EXPERIMENTAL RESULTS

In order to ensure that direct reaction theory is applicable to the experimental data, excitation curves for the 0^+ ground state and the first 2^+ excited state of ^{112}Cd, ^{118}Sn, and ^{128}Te were measured from an incident proton bombarding energy of about 15.5 to 16.1 MeV. In all cases there was no resonant behavior.

Differential cross sections were measured for proton elastic and inelastic scattering to the 0^+ ground state and the strongly excited 2^+ and 3^- collective states for ^{110,112,114,116}Cd, ^{112,116,118,120,122,124}Sn, and ^{126,128,130}Te. Figures 1, 2, and 3 show a comparison of the experimental differential cross sections for the cadmium, tin, and tellurium isotopes, respectively. From previous systematic studies of (p,p) and (p,p') differential cross sections at 16 MeV,[6] it is clear that all the isotopes display general characteristics of vibrational nuclei. That is, these angular distributions show marked diffraction-like structure, while those of rotational nuclei would exhibit a smoother pattern. The cross sections vary systematically with A, and have similar shapes for each type of state (0^+,2^+,3^-). The elastic angular distributions shift toward smaller angles and show increasing damping, both with increasing A. Furthermore, the magnitudes of the 2^+ and 3^- cross sections for each isotope are comparable and their angular distributions oscillate out of phase. The magnitudes of the inelastic cross sections decrease with increasing A. The integrated experimental cross sections $(1/2\pi)(\int_{\theta_1}^{\theta_2} d_\theta)$ for the 2^+ and 3^- states are plotted as a function of A in Figs. 4–7. (Note that the lower limit of integration for the 2^+ states of a given set of isotopes is usually not the same as that of the 3^- states.)

The 3^- integrated cross sections for ^{118}Sn and ^{120}Sn have been corrected for the contributions of 4^+ states at $Q=-2.28$ MeV in ^{118}Sn and at $Q=-2.35$ MeV in ^{120}Sn. These states, being approximately 50 keV from the 3^- states, were not resolved. The differential cross section has been measured for the 4^+ state in ^{120}Sn at $E_p=17.7$ MeV,[7] and the integrated cross section is 0.25 mb. The integrated cross section was extrapolated to 16 MeV by approximating the energy dependence of the cross section from the excitation curves for ^{118}Sn, and the corrected $\sigma_{4^+}=0.395$ mb. The 4^+ level in ^{118}Sn was assumed equal in strength to the 4^+ level in ^{120}Sn and the same value of σ_{4^+} was used for ^{118}Sn. This is a reasonable assumption since 11-MeV inelastic proton scattering shows the strength of these states to be similar.[8] The integrated cross sections of the 3^- states

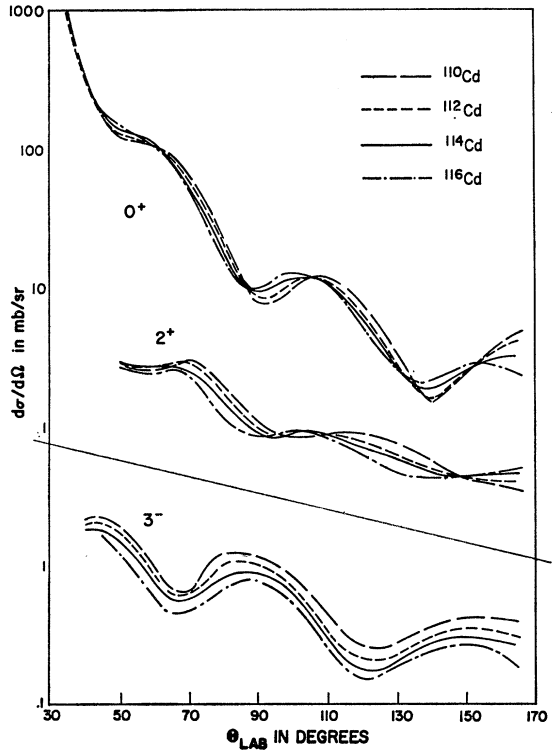

FIG. 1. Experimental (p,p) and (p,p') differential cross sections compared for the cadmium isotopes.

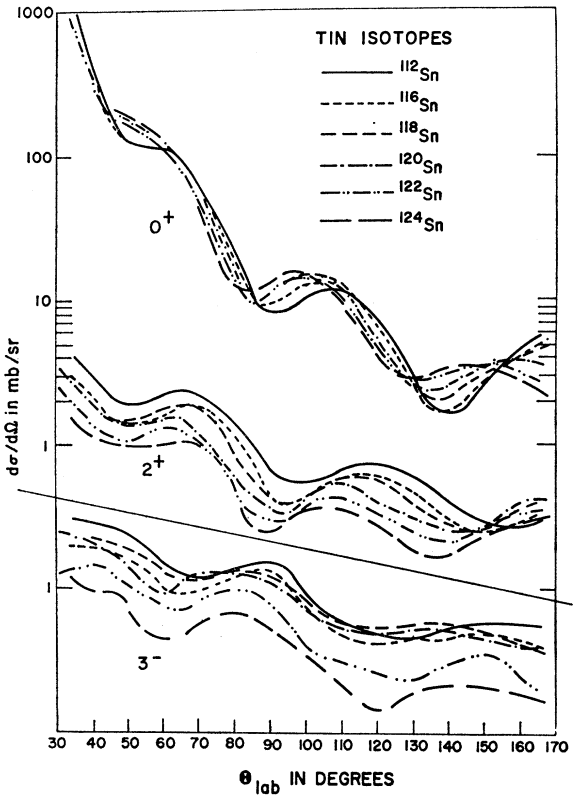

FIG. 2. Experimental (p,p) and (p,p') differential cross sections compared for the tin isotopes.

[6] See Ref. 5; and M. Slagowitz, P. Stoler, W. Makofske, W. Savin, H. Ogata, and T. H. Kruse (to be published).

[7] O. N. Jarvis, B. G. Harvey, D. L. Hendrie, and J. Mahoney Nucl. Phys. **A102**, 625 (1967).

[8] D. L. Allan, B. H. Armitage, and B. A. Doran, Nucl. Phys. **66**, 481 (1965).

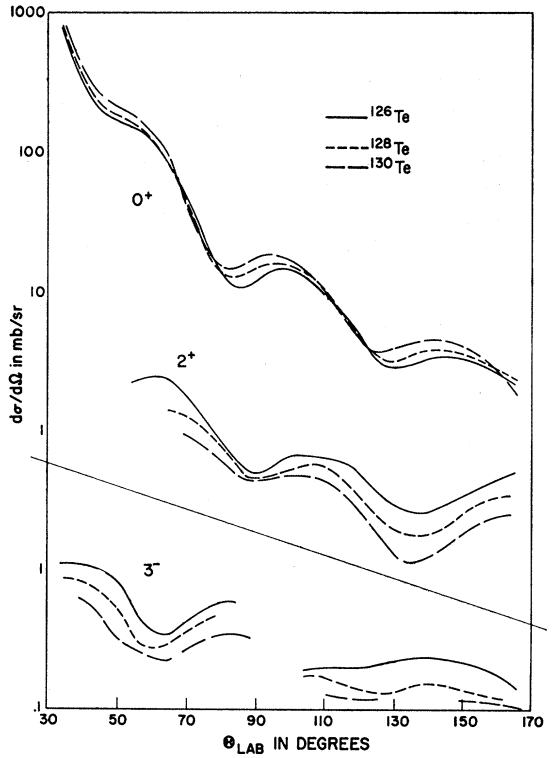

FIG. 3. Experimental (p,p) and (p,p') differential cross sections compared for the tellurium isotopes.

in ^{118}Sn and ^{120}Sn were reduced from 1.72 to 1.33 mb, and from 1.47 to 1.08 mb, respectively.

A possible explanation for the behavior of σ_{2^+} and σ_{3^-}, besides decreasing collectivity, is suggested by the elastic cross sections. In terms of the optical model, the increased damping of the oscillation amplitude is expected to occur if the surface imaginary potential gets deeper with increasing A.[9] However, as shown later, the net effect of optical-parameter variation on inelastic scattering is small.

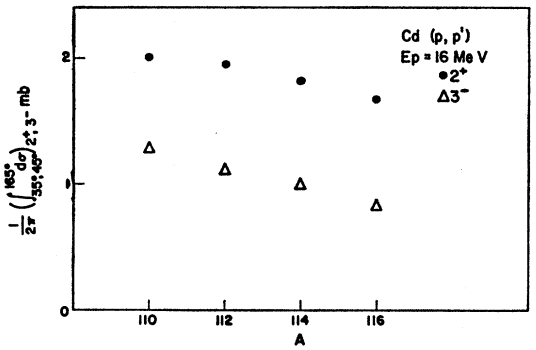

FIG. 4. Experimental integrated cross sections for inelastic scattering to the 2^+ and 3^- states plotted as a function of A for the cadmium isotopes.

IV. COMPARISON WITH THEORY

A. Optical-Model Analysis

The elastic scattering differential cross sections were fitted using an optical-model potential of the form

$$V(r) = -V(e^x+1)^{-1} + 4ia'W_D \frac{d}{dx'}(e^{x'}+1)^{-1} + \frac{(2\mathbf{l}\cdot\mathbf{s})}{r} V_s \frac{d}{dr}(e^{x_s}+1)^{-1} + V_c,$$

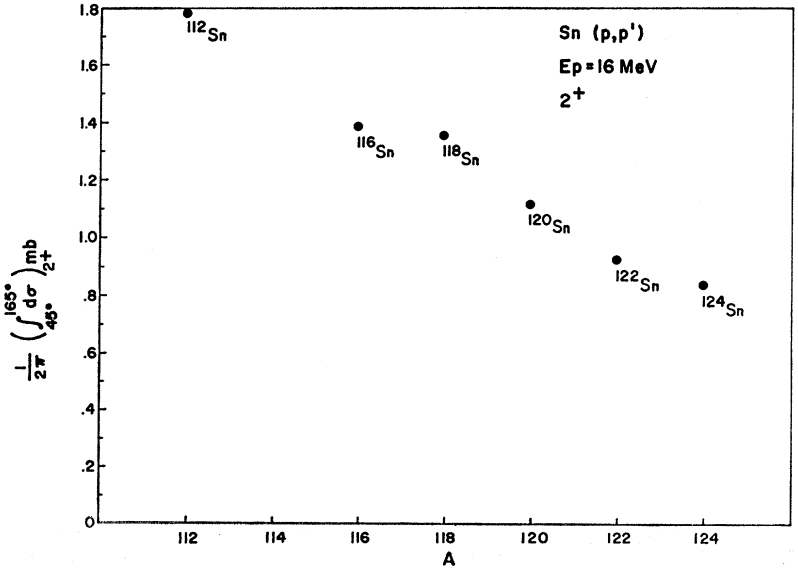

FIG. 5. Experimental integrated cross sections for inelastic scattering to the 2^+ state versus A for the tin isotopes.

[9] This explanation was suggested to us by G. W. Greenlees and T. Tamura.

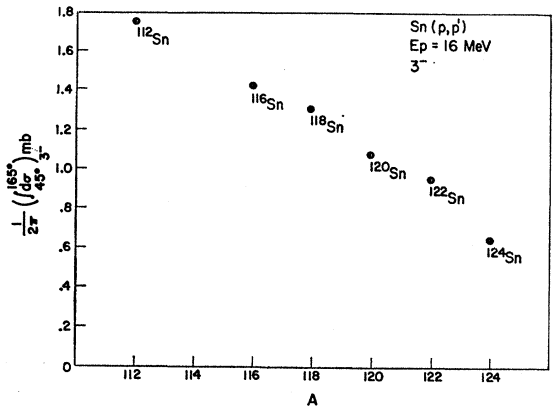

FIG. 6. Experimental integrated cross sections for inelastic scattering to the 3^- state versus A for the tin isotopes.

where

$$x=(r-r_0A^{1/3})/a, \quad x'=(r-r_0'A^{1/3})/a',$$

and

$$x_s=(r-r_sA^{1/3})/a_s.$$

The Coulomb potential V_c is that of a uniformly charged sphere of radius $1.2A^{1/3}$ fm.

The optical-model program OPTIX 1[10] incorporated an automatic parameter search code which minimizes

$$\chi^2=\sum_{i=1}^{N}\left[\frac{\sigma_{\rm th}(\theta i)-\sigma_{\rm expt}(\theta i)}{\Delta\sigma_{\rm expt}(\theta i)}\right]^2$$

with respect to any desired number of parameters.

The magnitude of the spin-orbit potential, the diffuseness, and the spin-orbit radius are known to have little effect on the differential cross section.[11] Thus, these parameters were held fixed at standard values for all the nuclei. ($V_s=6$ MeV, $a_s=0.7$ fm, and $r_s=1.1$ fm.)[12–14]

Since it was thought that a systematic variation of V and W_D might be exhibited by the isotopes of a given element, the geometrical parameters were fixed, and a search was made on V and W_D. Good over-all fits were found for the cadmium and tin isotopes with $r_0=1.2$ fm, $a=0.7$ fm, $r_0'=1.25$ fm, and $a'=0.65$ fm.[11] There are a few discrepancies in the quality of the fits. For example, the fit for ^{118}Sn with these geometrical parameters is poor, and the W_D is not systematic. The possibility that this could be attributed to an error in the absolute normalization was checked by doing another normalization on a different rolled ^{118}Sn target. This result agreed with the first normalization to within 2%. A third measurement using a thin evaporated ^{118}Sn target agreed, within the statistical errors, with the other two results. The reproducibility of the data leads us to conclude that the effect is real. There is also a slight divergence between calculations and experiment at back angles for ^{114}Cd and ^{116}Cd. Changing the two diffuseness parameters slightly ($a=0.725$ fm and $a'=0.625$ fm) reduced back-angle discrepancies, but the ^{110}Cd fit then became much worse.

The tellurium data could not be fit satisfactorily with the same geometrical parameters as those found for the cadmium and tin isotopes. An increase in the real diffuseness to 0.75 fm and a decrease in the imaginary diffuseness to 0.625 fm were necessary in order to obtain fairly good fits to all three tellurium isotopes.

Table I shows the optical-model parameters V and W_D for all the isotopes. The experimental errors used in the calculation of χ^2 were statistical in nature (1–3%). The systematic trends in the real and surface imaginary potentials are apparent except for ^{118}Sn and for V of ^{112}Sn.

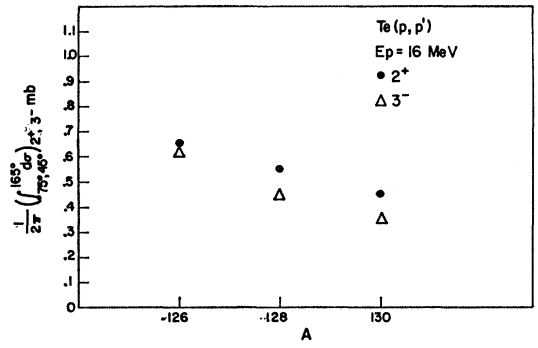

FIG. 7. Experimental integrated cross sections for inelastic scattering to the 2^+ and 3^- states versus A for the tellurium isotopes.

TABLE I. The real and surface imaginary parts (V and W_D) of the optical potential obtained by minimizing χ^2 for N data points under the stated geometrical restrictions. The reaction cross section σ_R calculated with these parameters is also given.

	V (MeV)	W_D (MeV)	σ_R (mb)	χ^2	χ^2/N
^{110}Cd	54.90	10.85	1202	234	9
^{112}Cd	55.06	11.16	1222	97	4
^{114}Cd	55.36	11.84	1246	186	7
^{116}Cd	55.77	12.45	1269	183	7
^{112}Sn	55.46	10.38	1166	850	34
^{116}Sn	55.25	10.73	1199	733	29
^{118}Sn	55.28	11.83	1229	680	27
^{120}Sn	55.79	11.52	1239	128	5
^{122}Sn	56.14	11.75	1256	335	13
^{124}Sn	56.37	12.22	1277	569	23
^{126}Te	55.41	13.28	1275	452	17
^{128}Te	55.87	13.46	1291	446	17
^{130}Te	56.14	14.49	1315	190	7

[10] C. F. Moore and P. Richard, Florida State University, Technical Report No. 8, 1965 (unpublished).
[11] R. L. Robinson, J. L. C. Ford, Jr., P. H. Stelson, and G. R. Satchler, Phys. Rev. **146**, 816 (1966).
[12] L. Rosen, J. G. Beery, and A. S. Goldhaber, Ann. Phys. (N. Y.) **34**, 96 (1965).
[13] G. W. Greenlees and G. J. Pyle, Phys. Rev. **149**, 836 (1966).
[14] G. R. Satchler, Nucl. Phys. **A92**, 273 (1967).

The comparison of the optical-model calculations with the experimental elastic scattering differential cross sections is shown in Figs. 8–20. The solid lines represent the theoretical results, while the points represent the measured cross sections. The errors are generally less than the size of the points.

If the systematic variation of V and W_D is attributed to an isospin dependence in the optical potential, the strength of the symmetry term $(N-Z)/A$ in both the real and imaginary parts may be extracted. Before plotting the real well depth V as a function of $(N-Z)/A$ a variation with A arising out of the variation of the Coulomb potential with Z must be subtracted from V. This term is taken to be $0.4\,Z/A^{1/3}$.[15] The cadmium and tin data are plotted separately from the tellurium data since their geometrical parameters are different. Figures 21 and 22 show the corrected real well depth versus $(N-Z)/A$. A least-squares fit to the data gives the strength of the symmetry term as 16 MeV (Cd and Sn), and 27 MeV (Te). The linear correlation of W_D with $(N-Z)/A$ is shown in Figs. 23 and 24. The symmetry strengths were 23 MeV (Cd and Sn) and 44 MeV (Te). Both real and imaginary strengths are in reasonable

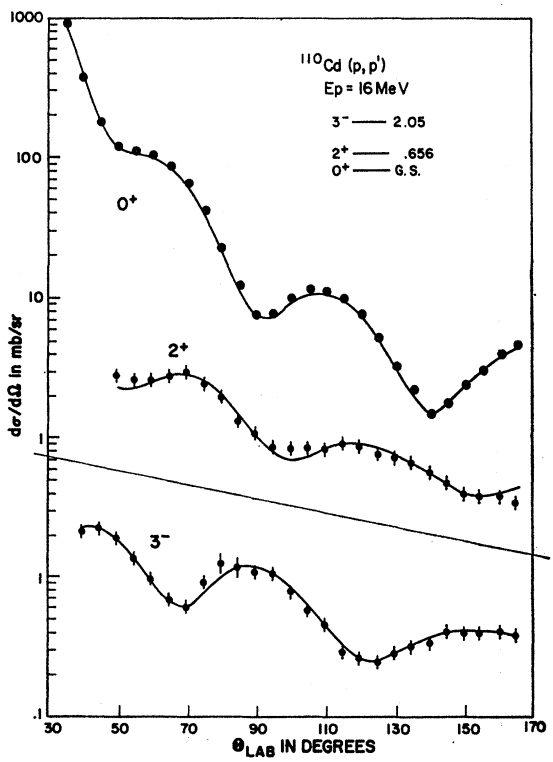

FIG. 8. Differential cross sections for ^{110}Cd. The experimental elastic cross sections are compared with the optical-model calculation using the parameters of Table I. The experimental inelastic 2^+ and 3^- cross sections are compared with the normalized theoretical predictions of the distorted-wave calculation.

[15] F. G. Perey, Phys. Rev. 131, 745 (1963).

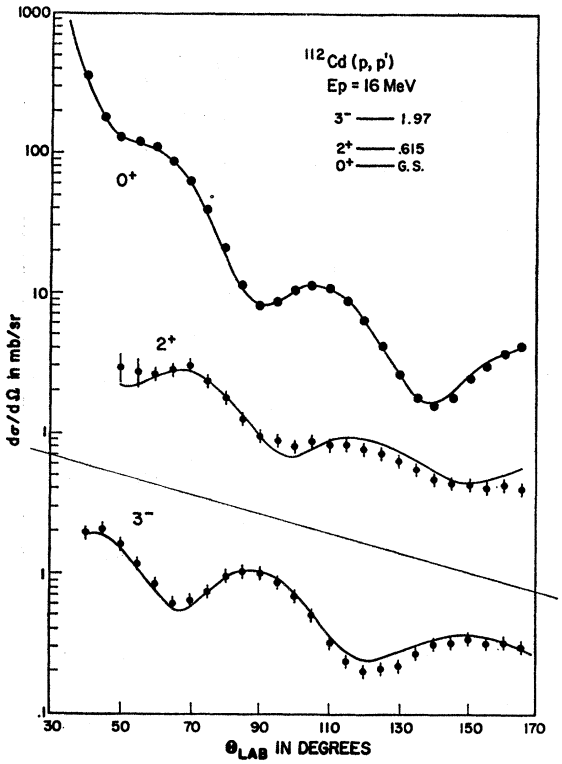

FIG. 9. Differential cross sections for ^{112}Cd. See also caption for Fig. 8.

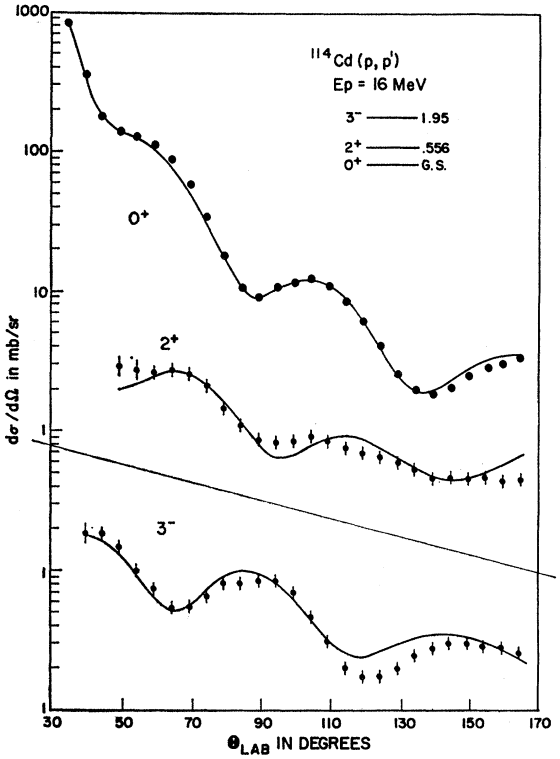

FIG. 10. Differential cross sections for ^{114}Cd. See also caption for Fig. 8.

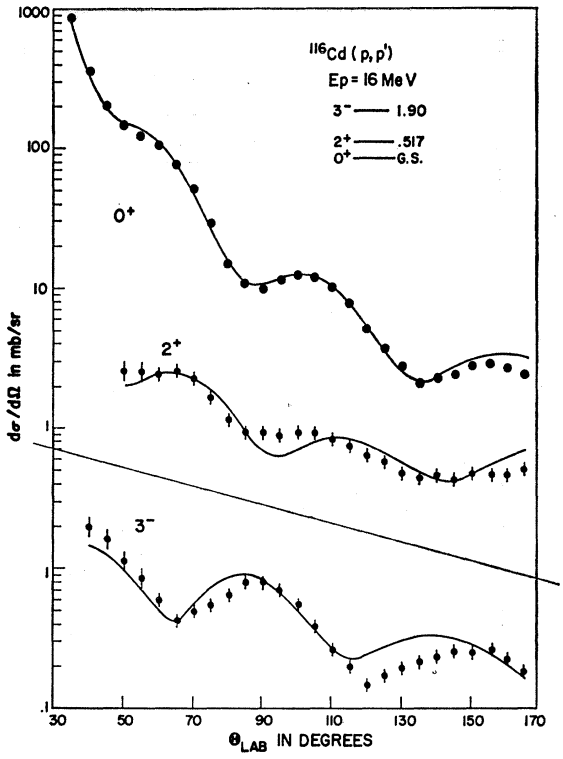

FIG. 11. Differential cross sections for ^{116}Cd. See also caption for Fig. 8.

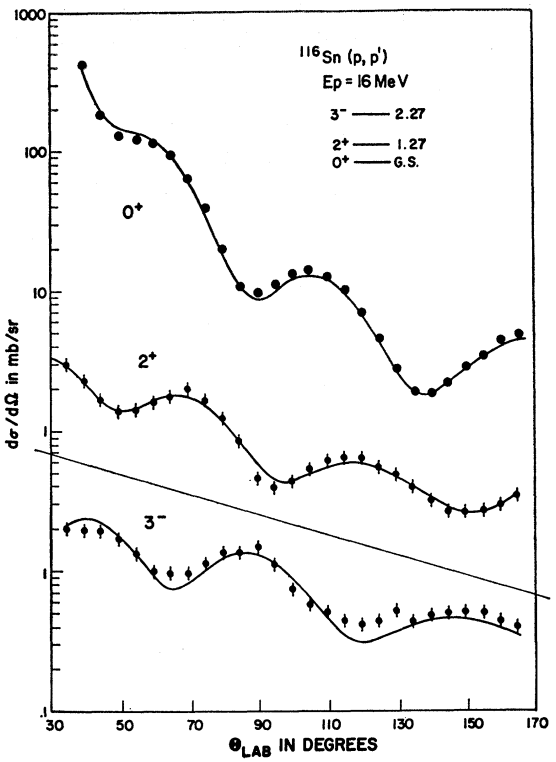

FIG. 13. Differential cross sections for ^{116}Sn. See caption for Fig. 8.

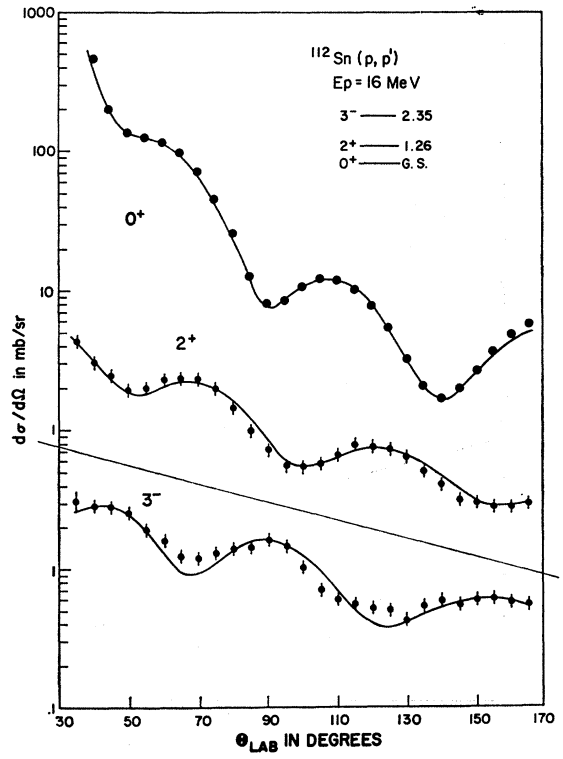

FIG. 12. Differential cross sections for ^{112}Sn. See also caption for Fig. 8.

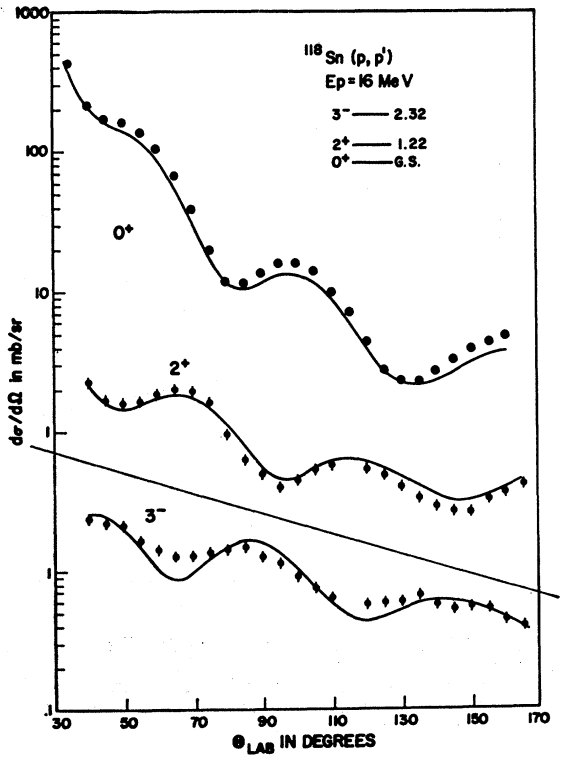

FIG. 14. Differential cross sections for ^{118}Sn. See caption for Fig. 8.

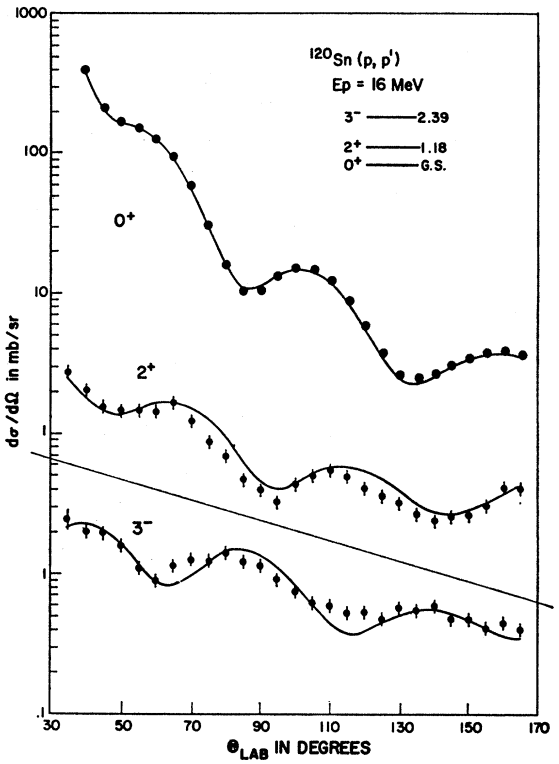

FIG. 15. Differential cross sections for ^{120}Sn. See caption for Fig. 8.

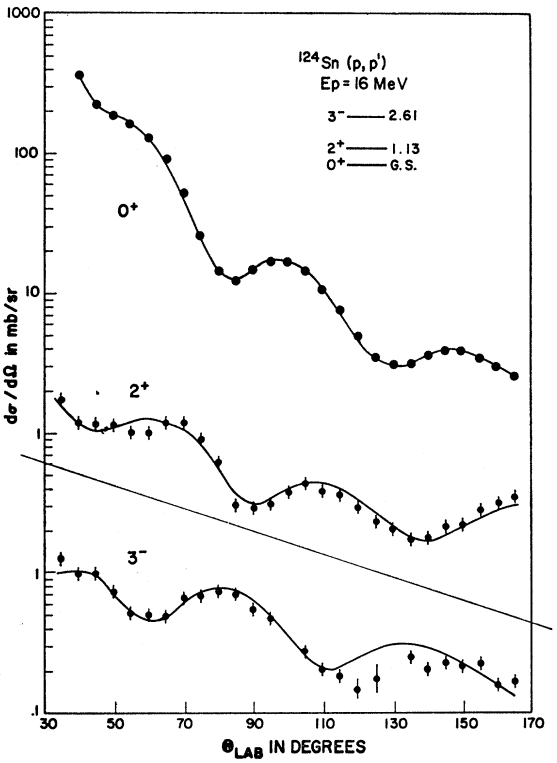

FIG. 17. Differential cross sections for ^{124}Sn. See caption for Fig. 8.

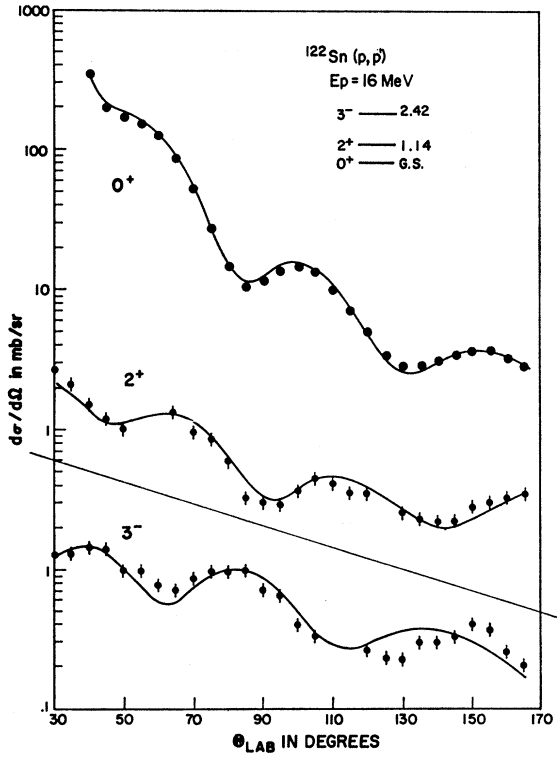

FIG. 16. Differential cross sections for ^{122}Sn. See caption for Fig. 8.

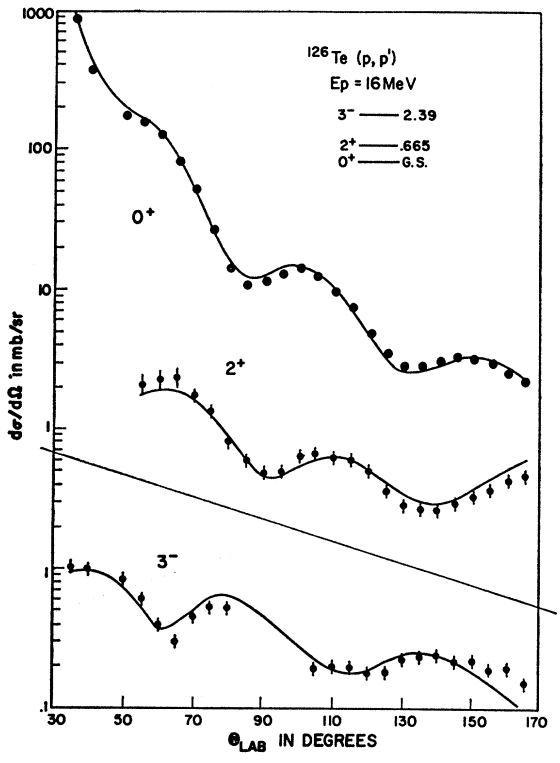

FIG. 18. Differential cross sections for ^{126}Te. See caption for Fig. 8.

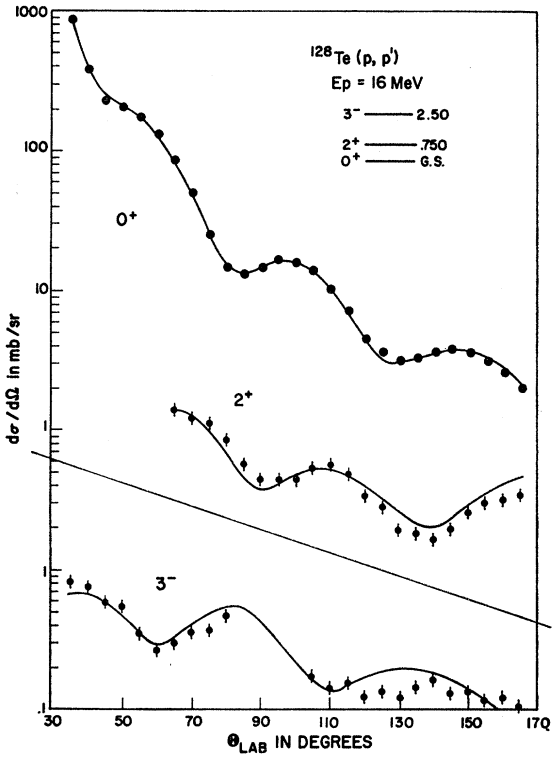

FIG. 19. Differential cross sections for ^{128}Te. See caption for Fig. 8.

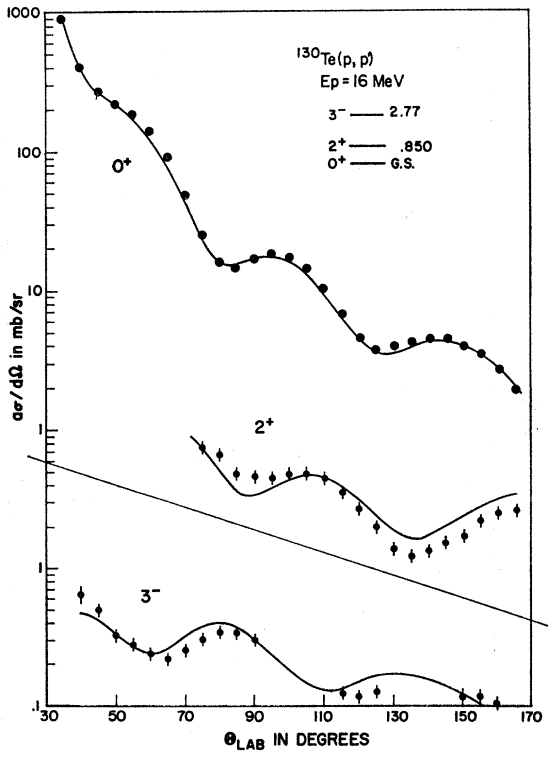

FIG. 20. Differential cross sections for ^{130}Te. See caption for Fig. 8.

agreement with values extracted from proton scattering data and other empirical evidence.[15–17]

Table I also shows the total proton reaction cross sections σ_R calculated by the optical-model program with the best-fit parameters of this section. An increasing magnitude with increasing A is evident. σ_R data on ^{116,118,120}Sn at 14.5 MeV have values of 1113±45, 1194±29, and 1152±34 mb, respectively.[18] These experimental values are larger than the optical-model predictions at 14.5 MeV and are, in fact, quite close to the values in Table I.

B. Distorted-Wave Analysis

The calculations for the inelastic scattering were carried out with the Fortran distorted-wave program DWUCK.[19] These computations, utilizing the zero-range approximation and including Coulomb excitation, were made assuming the collective vibrational model for the interaction potential. A complex interaction was used

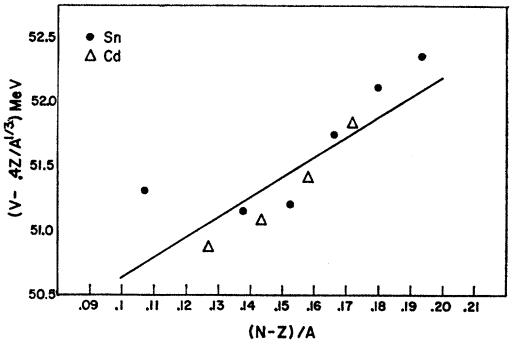

FIG. 21. The corrected real well depth as a function of $(N-Z)/A$ for the cadmium and tin isotopes. The least-squares fit gives a symmetry strength of 16 MeV.

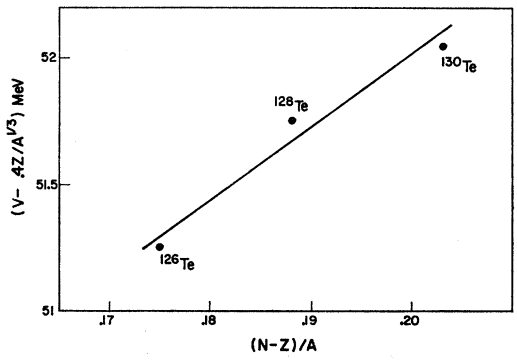

FIG. 22. The corrected real well depth as a function of $(N-Z)/A$ for the tellurium isotopes. The least-squares fit gives a symmetry strength of 27 MeV.

[16] P. E. Hodgson, Phys. Letters 3, 352 (1963).
[17] P. Kossanyi-Demay, R. de Swiniarski, and C. Glashausser, Nucl. Phys. A94, 513 (1967).
[18] J. F. Dicello, G. J. Igo, and M. L. Roush, Phys. Rev. 157, 1001 (1967).
[19] DWUCK is a distorted-wave Fortran program obtained from P. D. Kunz of the University of Colorado.

implying that both the real and imaginary parts of the optical potential are allowed to be nonspherical with equal deformabilities for each part.

The theoretical inelastic cross sections were normalized to the experimental cross sections in order to extract the square of the deformation parameters. This extraction process was performed in three ways. The first method consisted of multiplying each theoretical cross section by the same factor, and then comparing this with the experimental differential cross section, minimizing

$$\chi^2=\sum_{i=1}^{N}\left[\frac{\beta_i^2\sigma_{\mathrm{DWUCK}}(\theta i)-\sigma_{\mathrm{expt}}(\theta i)}{\Delta\sigma_{\mathrm{expt}}(\theta i)}\right]^2.$$

Table II shows the deformation parameters thus obtained for the Cd, Sn, and Te collective 2^+ and 3^- states. The errors shown are determined from the statistical errors assigned to the experimental cross sections and do not reflect absolute normalization uncertainties nor uncertainties associated with the theoretical calculation.

The second method of β_i extraction compares the experimental and theoretical integrated cross sections over the measured angular range. If the angular distributions of the experimental and calculated cross sections are close, one would expect this method to give the same results as the first. In fact, for almost all the isotopes, the change in the deformation parameters is less than 3%. (The β_3's given for ^{118}Sn and ^{120}Sn were obtained by comparing the theoretical and experimental integrated cross sections. The measured results were corrected for the contribution of a known 4^+ state in each instance.)

Since the back angles in the calculated inelastic scattering are more sensitive to changes in the optical-model parameters, the deformation parameters were extracted using the first method by considering only the forward-angle data ($\theta<120°$). The β's found in this way were within 1% of those extracted using all the angles. No essential differences were found in these three methods.

Figures 8–20 show a comparison of the normalized theoretical and experimental 2^+ and 3^- cross sections. The 3^- states of ^{118}Sn and ^{120}Sn in Figs. 14 and 15 contain 4^+ contributions.

The following systematic trends are observed in the deformation parameters. The β_2's and β_3's for the cadmium, tin, and tellurium isotopes decrease with increasing A, indicating a decreasing collectivity for these states. The only exception is ^{118}Sn, which exhibits nonsystematic behavior. Since the optical-model fit for ^{118}Sn with the standardized geometrical parameters is poor, a different set which gave a good fit was used in the DWUCK program. These parameters were $r_0=1.2$ fm,

TABLE II. The energy, spin, and parity of the collective 2^+ and 3^- states with the deformation parameters obtained from the proton scattering.

	Level (MeV)	I^π	Deformation parameter
^{110}Cd	0.656	2^+	0.175±0.010
	2.05	3^-	0.175±0.013
^{112}Cd	0.615	2^+	0.173±0.011
	1.97	3^-	0.164±0.011
^{114}Cd	0.556	2^+	0.169±0.010
	1.95	3^-	0.160±0.012
^{116}Cd	0.517	2^+	0.165±0.011
	1.90	3^-	0.149±0.014
^{112}Sn	1.26	2^+	0.152±0.010
	2.35	3^-	0.203±0.010
^{116}Sn	1.27	2^+	0.133±0.010
	2.27	3^-	0.185±0.010
^{118}Sn[a]	1.22	2^+	0.134±0.010
	2.32	3^-	0.168±0.014[b]
^{120}Sn	1.18	2^+	0.119±0.010
	2.39	3^-	0.159±0.020[b]
^{122}Sn	1.14	2^+	0.112±0.007
	2.42	3^-	0.152±0.014
^{124}Sn	1.13	2^+	0.108±0.007
	2.61	3^-	0.133±0.020
^{126}Te	0.665	2^+	0.139±0.008
	2.39	3^-	0.131±0.010
^{128}Te	0.750	2^+	0.124±0.008
	2.50	3^-	0.110±0.010
^{130}Te	0.850	2^+	0.117±0.007
	2.77	3^-	0.100±0.012

[a] Calculated with a parameter set giving a good fit to the elastic scattering.
[b] Determined by comparing experimental and theoretical integrated cross sections.

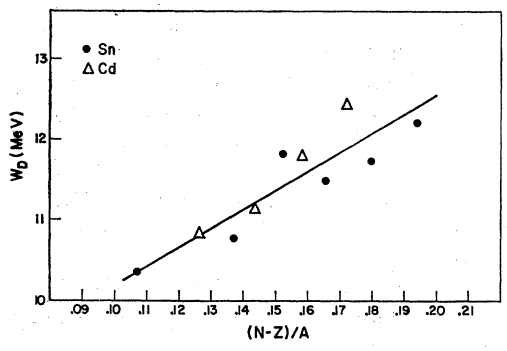

FIG. 23. The surface imaginary well depth as a function of $(N-Z)/A$ for the cadmium and tin isotopes. The least-squares fit gives a symmetry strength of 23 MeV.

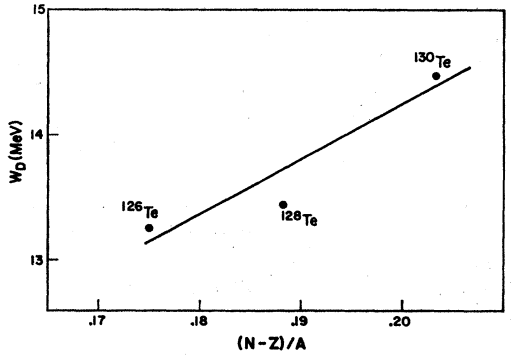

FIG. 24. The surface imaginary well depth as a function of $(N-Z)/A$ for the tellurium isotopes. The least-squares fit gives a symmetry strength of 44 MeV.

$a=0.65$ fm, $r_0'=1.25$ fm, and $a'=0.7$ fm. The minimum χ^2 was found at $V=55.78$ MeV and $W_D=9.66$ MeV. The deformation parameters obtained were $\beta_2=0.134$ and $\beta_3=0.168$, as opposed to the poor-fit values of $\beta_2=0.142$ and $\beta_3=0.182$. Since the validity of the theoretical calculation depends upon a good approximation to the elastic scattering, the first set of deformation parameters is quoted in Table II.

In Table III the theoretical and experimental integrated inelastic cross sections are shown for each 2^+ and 3^- state. The range of integration is the same for each state in a given group of isotopes. The variation of the theoretical integrated cross sections (calculated assuming $\beta_l=1$) for a particular state in a given set of isotopes is not large. This small variation shows that the decrease in the measured inelastic cross sections with increasing A can be accounted for almost entirely by decreasing collectivity. For medium-energy protons the inelastic cross section in the DWBA is roughly proportional to $1/W_D^2$. This dependence comes from the additional damping imposed on the distorted waves in the vicinity of the nuclear surface. Increases in V tend to have the opposite effect and reduce the effect of increasing W_D alone.[20]

These results may be compared with the results of a coupled-channel calculation for the 0^+–2^+ states of ^{112}Sn and ^{124}Sn in which the β_2's were taken from Coulomb excitation results.[21] Including the 2^+ state in the calculation reduces the value of W_D from that needed to fit only the elastic scattering. The final values of W_D were 11.48 MeV for ^{112}Sn and 15.53 MeV for ^{124}Sn. This large W_D variation was necessary because the variation in collectivity between ^{112}Sn and ^{124}Sn obtained from Coulomb excitation is less than that obtained from proton scattering. Using β_l values derived from the distorted-wave analysis, the A dependence of inelastic scattering cross sections appears to be substantially explained by collectivity variation; the net effect of variation of V and W_D is small. With our geometrical assumption, a V and W_D variation is necessary to describe the variation in elastic scattering cross sections. It is clear that the strength of the symmetry term in the imaginary part of the optical potential would become larger if a coupled-channel calculation were performed for all the Cd, Sn, and Te isotopes, since the deformation parameters decrease with increasing A.

TABLE III. Experimental inelastic integrated cross sections for the 2^+ and 3^- states with the theoretical inelastic integrated cross sections ($\beta_l=1$) obtained from the distorted-wave calculation.

	$(\sigma_2{}^+)_{\text{expt}}$ (mb)	$(\sigma_2{}^+)_{\text{DWUCK}}$ (mb)	$(\sigma_3{}^-)_{\text{expt}}$ (mb)	$(\sigma_3{}^-)_{\text{DWUCK}}$ (mb)
^{110}Cd	2.02±0.02	65.49	1.29±0.03	41.99
^{112}Cd	1.96±0.03	65.82	1.11±0.02	41.65
^{114}Cd	1.82±0.02	63.70	0.99±0.02	40.14
^{116}Cd	1.67±0.03	62.09	0.82±0.02	39.58
^{112}Sn	1.84±0.01	79.60	1.84±0.01	43.37
^{116}Sn	1.45±0.01	80.68	1.49±0.01	43.33
^{118}Sn	1.46±0.01	73.75[a]	1.33±0.03	39.81[a]
		81.31[b]		47.12[b]
^{120}Sn	1.11±0.02	80.16	1.08±0.03	42.12
^{122}Sn	0.92±0.01	81.16	0.98±0.02	42.71
^{124}Sn	0.87±0.01	79.82	0.67±0.03	42.28
^{126}Te	0.65±0.01	35.04	0.62±0.01	38.88
^{128}Te	0.55±0.01	34.06	0.45±0.01	39.84
^{130}Te	0.45±0.01	31.49	0.35±0.01	38.57

[a] Calculated with the standardized geometrical parameters.
[b] Calculated with a parameter set giving a good fit to the elastic scattering:

$$(\sigma_2{}^+)=\frac{1}{2\pi}\int_{\theta_1}^{\theta_2}(d\sigma_2{}^+),$$

$$(\sigma_3{}^-)=\frac{1}{2\pi}\int_{\theta_3}^{\theta_4}(d\sigma_3{}^-).$$

Calculations were performed in order to ascertain the effect of parameter uncertainties in the calculated inelastic scattering. Since polarization experiments have not been performed on these isotopes at 16 MeV, there is ambiguity in the magnitude of the spin-orbit potential. The optical-model fit was essentially unchanged by using $V_s=7$ MeV instead of 6 MeV and keeping all the other parameters the same. The DWUCK program was run with both sets of parameters for a typical nucleus ^{122}Sn. For $V_s=6$ MeV, $\beta_2=0.1117$ and $\beta_3=0.1520$, while for $V_s=7$ MeV, $\beta_2=0.1119$ and $\beta_3=0.1521$. Thus it is clear that the spin-orbit magnitude uncertainty will not affect the deformation parameters significantly.

The effect on the deformation parameters of different optical-model parameters which give essentially the same fits for elastic scattering was tested by using a different set for ^{124}Sn($V=54.6$ MeV, $W_D=16.3$ MeV, $V_s=7.5$ MeV, $a=a_s=0.625$ fm, $r_0=r_s=1.25$ fm, $a'=0.580$ fm, $r_0'=1.17$ fm) in the DWUCK program. The values of β obtained were not changed significantly (1–2%).

It is preferable to compare experiments in terms of deformation lengths ($\delta_l=\beta_l R$).[22] The δ_l's are physically meaningful because they enter directly into the expansion of the potential. Values of R in electromagnetic experiments differ from those which appear in the inelastic scattering of strongly interacting projectiles. Optical-model fits to the elastic scattering often contain ambiguities for the radius.

Figure 25 shows a comparison of deformation lengths for the cadmium isotopes. The δ_2 values are fairly close in magnitude, although they show different systematic trends for the two types of measurements. Coulomb excitation data[23] show an increasing magnitude with increasing A, while (p,p') values decrease. These trends are real within the estimated errors in both cases. Both the (p,p') and Coulomb excitation[24] δ_3 values show a decreasing magnitude with increasing A.

In Fig. 26, a comparison is made of deformation

[20] F. G. Perey and G. R. Satchler, Phys. Letters **5**, 212 (1963).
[21] W. Makofske, M. Slagowitz, W. Savin, H. Ogata, T. H. Kruse, and T. Tamura, Phys. Letters **25B**, 322 (1967).
[22] N. Austern and J. S. Blair, Ann. Phys. (N.Y.) **33**, 32 (1965).
[23] P. H. Stelson and L. Grodzins, Nucl. Data **1**, No. 1 (1965).
[24] F. K. McGowan, R. L. Robinson, P. H. Stelson, and J. L. C. Ford, Jr., Nucl. Phys. **66**, 97 (1965).

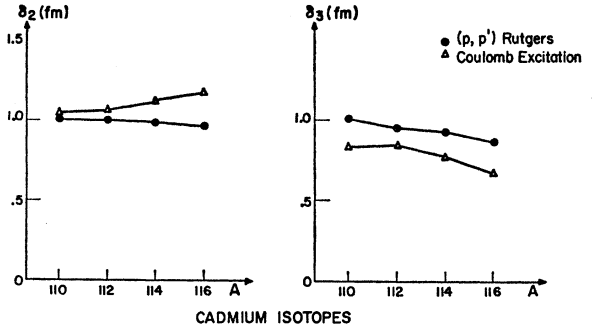

FIG. 25. The deformation lengths ($\delta_l=\beta_l R$) for the cadmium isotopes obtained in the present work compared with Coulomb excitation results.

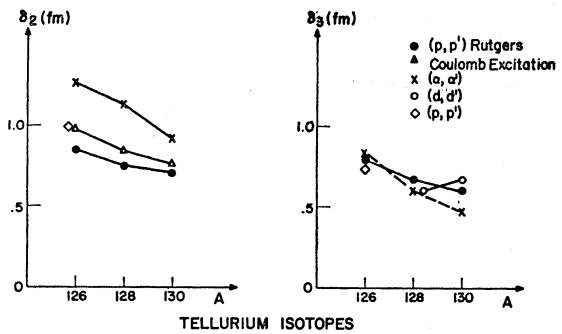

FIG. 27. The deformation lengths ($\delta_l=\beta_l R$) for the tellurium isotopes obtained in the present work compared with the results of other types of measurements.

lengths for the tin isotopes. The Coulomb excitation measurements for δ_2[23] are clearly smaller than those extracted from proton scattering for ^{112}Sn to ^{118}Sn. The δ_3's extracted from Coulomb excitation experiments[25] are in fair magnitude agreement with the proton results.

Deformation lengths have been extracted at Saclay from 44-MeV (α,α') scattering using the Austern and Blair model.[26] These δ_2's are in agreement with Coulomb excitation values, while the δ_3's are much lower than those obtained by any other technique. Other (α,α') scattering yields deformation lengths with the use of a DWBA calculation.[27] The δ_2 values differ from those obtained from (α,α') scattering at Saclay. The δ_3's lie close to the Coulomb excitation and the (p,p') measurements.

Recent results from 150-MeV electron scattering (e,e') on ^{116}Sn, ^{120}Sn, and ^{124}Sn [Ref. 28] show relatively low values for δ_2 and δ_3.

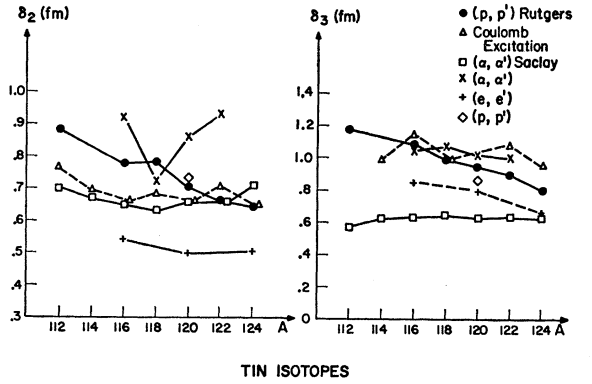

FIG. 26. The deformation lengths ($\delta_l=\beta_l R$) for the tin isotopes obtained in the present work compared with the results of other types of measurements.

Another (p,p') result[7] for ^{120}Sn gives a δ_2 value which agrees well with the present result. Their δ_3 value is lower, but there is agreement within the estimated errors.

Figure 27 shows a comparison of δ_2 and δ_3 values for the tellurium isotopes. The Coulomb-excitation[23] and (α,α')[29] δ_2 values show a very similar trend with increasing A. This decreasing behavior is also exhibited by the (p,p') results. The δ_3's extracted from (α,α') data show a greater variation than the (p,p') values. Two (d,d')[30] and other (p,p') values[31] are in good agreement with the present proton data.

In Fig. 28 a comparison of theoretical values of $B(E2)$ and $B(E3)$ for the tin isotopes[32–36] is made with

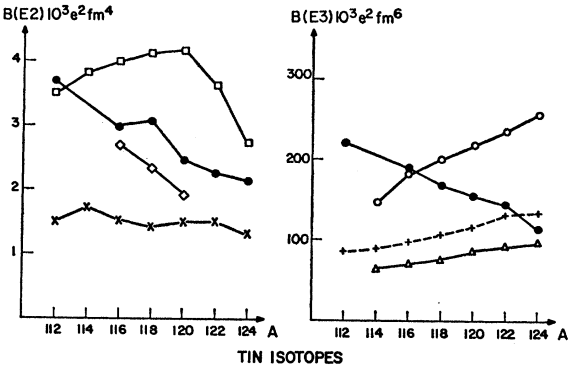

FIG. 28. Theoretical $B(E2)$ and $B(E3)$ values for the tin isotopes compared with those calculated from deformation parameters obtained from proton scattering. ●, (p,p') Rutgers; □, Ref. 32; ×, Ref. 33; △, Ref. 34 (BZ3); ○, Ref. 34 (BA3); +, Ref. 35; ◇, Ref. 36.

[25] D. G. Alkhazov, Yu. P. Gangzskii, I. Uh. Lemberg, and Yu. I. Udralov, Izv. Akad. Nauk SSSR **28**, 149 (1965).
[26] G. Bruge, J. C. Faivre, H. Faraggi, G. Vallois, A. Bussiere, and P. Rousel, Phys. Letters **22**, 654 (1966).
[27] N. Baron, R. F. Leonard, J. L. Need, W. M. Steward, and V. A. Madsen, Phys. Rev. **146**, 861 (1966).
[28] P. Barreau and J. B. Bellicard, Phys. Rev. Letters **19**, 1444 (1967).
[29] R. F. Leonard, W. M. Stewart, and N. Baron, Phys. Rev. **162**, 1125 (1967).
[30] Y. S. Kim and B. L. Cohen, Phys. Rev. **142**, 788 (1966).
[31] G. C. Pramila, R. Middleton, T. Tamura, and G. R. Satchler, Nucl. Phys. **61**, 448 (1965).
[32] L. Kisslinger and R. A. Sorenson, Rev. Mod. Phys. **35**, 853 (1963).
[33] S. Yoshida, Nucl. Phys. **38**, 380 (1962).
[34] R. J. Lombard and X. Campi-Benet, IPNO/TH-42, Orsay, 1965 (unpublished).
[35] C. J. Veje, Kgl. Danske Videnskab, Mat. Fys. Medd. **35**, 1 (1966).
[36] R. Raj, Y. K. Gambhir, and M. K. Pal., Phys. Rev. **163**, 1004 (1967).

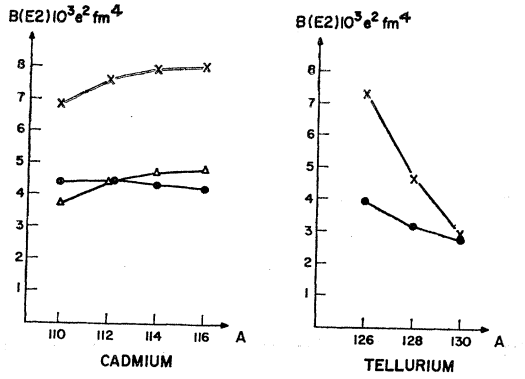

FIG. 29. Theoretical $B(E2)$ values for the cadmium and tellurium isotopes compared with those calculated from deformation parameters obtained from proton scattering. ●, Rutgers; △, Ref. 33; ×, Ref. 32.

values extracted from the (p,p') deformation parameters using

$$B(EI)=[(3/4\pi)ZR^I\beta_I]^2.$$

This relation assumes a uniform charge distribution out to the distance $R(\theta,\phi)$ and zero charge beyond. It is valid in the limit of small deformations. Although in general the agreement with the (p,p') data is not good, the most recent values for the $B(E2)$'s of ^{116,118,120}Sn, calculated by a modified Tamm-Dancoff approximation and assuming a pairing plus quadrupole interaction, indicate a decreasing trend with increasing A.[36] The predicted $B(E3)$ values all increase monotonically with increasing A while the experimental results indicate a decreasing trend.

Figure 29 shows a similar comparison for the $B(E2)$'s of the cadmium and tellurium isotopes.[32,33] For cadmium, the theoretical trend is opposite to the (p,p') experimental trend (but in agreement with Coulomb excitation measurements). For tellurium, the theoretical values show a rapidly decreasing magnitude with increasing A.

V. DISCUSSION

Although previous systematic optical-model analyses of proton scattering data have shown an increasing real well depth as a function of mass number, recent analyses of proton scattering and polarization data at 11 MeV have raised serious questions about the isospin dependence in the real part of the potential.[37]

A comparison of neutron and proton scattering, including nonelastic and total cross sections, has given some evidence for a complex potential term proportional to $\mathbf{t}\cdot\mathbf{T}$.[38] However, because of the accuracy of the neutron data, such conclusions are not without question at this time.

Recent work in which the optical model is reformulated has been successful in fitting proton elastic scattering data with two fewer parameters.[39] This model avoids geometrical assumptions and relates its parameters to quantities of more direct physical significance. Thus, the real parts of the potential are derived from the nuclear matter distribution and components of the nucleon-nucleon force.

In the analysis carried out in this paper, the assumptions of fixing the geometrical parameters and setting the radii proportional to the cube root of A clearly constrain the parameter space and allow variations in the potential well depths to be exhibited. For example, a diffuseness parameter a' which increases for heavier nuclei would lead to a less strong dependence of W_D on $(N-Z)/A$. The assumption of only a surface absorption term leads to a stronger dependence of W_D on $(N-Z)/A$ than would occur if a volume absorption term were also included.[38]

The deviations between the deformation lengths extracted from various experiments are not great considering the simplicity of the collective vibrational model. Although this model is a good approximation for the one-phonon collective states, there are discrepancies between theory and experiment for the two-phonon triplet states, electromagnetic transition probabilities, and quadrupole moments.[40] It is possible that the deformation of the nucleus leading to inelastic particle scattering may be different from the deformation of the charge distribution. It would be interesting to see if a difference in trend for the deformation parameters extracted from Coulomb excitation and (p,p') scattering experiments exists for other isotopes.

Inelastic α scattering on the calcium isotopes has shown that the higher 3^- octupole states are strongly excited and that the total 3^- strength decreases with A with increasing fractionization.[41] Such a correlation with higher 3^- states does not appear significant for the tin isotopes since (α,α') scattering shows these states to be very weakly excited.[42]

VI. CONCLUSION

The systematic damping of the elastic scattering angular distributions with increasing A may be interpreted in terms of increasing W_D variation. Optical-model fits assuming fixed geometrical parameters show that V and W_D increase with A. These results are consistent with an isospin dependence in both the real and surface imaginary parts of the optical potential. The magnitudes of the symmetry terms in the real and imaginary parts of the optical potential extracted in this work are in reasonable agreement with values obtained from other analyses.

[37] C. M. Perey and F. G. Perey, Phys. Letters **26B**, 123 (1968).
[38] G. R. Satchler, Nucl. Phys. **A91**, 75 (1967).
[39] G. W. Greenlees, G. J. Pyle, and Y. C. Tang, Phys. Rev. Letters **17**, 33 (1966); Phys. Rev. **171**, 1115 (1968).
[40] D. A. Bromley and J. Weneser, Comments Nucl. Particle Phys. **1**, 75 (1967).
[41] E. P. Lippincott and A. M. Bernstein, Phys. Rev. **163**, 1170 (1967).
[42] J. Alster (private communication).

The differential cross sections for inelastically scattered protons to the first 2^+ and 3^- states were found to be adequately explained by a distorted-wave calculation, assuming a collective vibrational model including complex coupling and Coulomb excitation. The large decreasing trends with increasing A observed in the inelastic cross sections are primarily accounted for by a decreasing collectivity. The deformation parameters deduced from these calculations are generally in agreement with those obtained from Coulomb excitation and other types of studies. Some differences arise, however, and further work in this area is desirable.

Note added in manuscript.

(1) Recent accurate results ($\pm 2\%$ relative errors) for $B(E2)$ values from Coulomb excitation of the even tin isotopes indicate a larger range of collectivity between ^{112}Sn and ^{124}Sn than shown by previous measurements [P. H. Stelson, F. K. McGowan, R. L. Robinson, W. T. Milner, and R. O. Sayer, Phys. Rev. **170**, 1172 (1968)]. This supports our conclusion that the differences in the 2^+ integrated cross sections for ^{112}Sn and ^{124}Sn are accounted for by a collectivity difference. Assuming a realistic rounded charge distribution with $r_0=1.07$ fm and $a=0.55$ fm [L. W. Owen and G. R. Satchler, Nucl. Phys. **51**, 155 (1964)] increases the Coulomb excitation β_2's by approximately 10%, so that the proton scattering and Coulomb excitation results agree on the average within 3%.

(2) Further optical-model analysis of the proton data, searching on the real central potential parameters V, r_0, and a, indicates that the volume integral of the real part of the potential divided by A and plotted against $(N-Z)/A$ (see Ref. 39) is consistent with a zero or small positive slope.

(3) A similar plot, obtained by searching on the six parameters in the real and imaginary parts of the optical potential, shows no definite slope. When the same analysis is applied to the imaginary part of the potential, the imaginary volume integral divided by A and plotted against $(N-Z)/A$ exhibits a positive slope in both cases.

ACKNOWLEDGMENTS

We wish to thank P. D. Kunz for providing us with the distorted-wave program DWUCK and helpful comments on its use. We are grateful for useful conversations with G. W. Greenlees and T. Tamura.

PHYSICAL REVIEW VOLUME 174, NUMBER 4 20 OCTOBER 1968

Levels in Even-Even Hg^{192}, Hg^{194}, Hg^{196}, and Hg^{198}†

R. F. PETRY,* R. A. NAUMANN,‡ AND J. S. EVANS§
Palmer Physical Laboratory, Frick Chemical Laboratory, and Princeton-Pennsylvania Accelerator, Princeton University, Princeton, New Jersey 08540

(Received 28 March 1968)

The decay of the 2^- and 7^+ isomeric states of Tl^{192}, Tl^{194}, Tl^{196}, and Tl^{198} has been studied, using isotopically separated sources produced by high-energy proton spallation of lead and uranium targets. γ-ray and conversion-electron spectra have been recorded, and extensive coincidence measurements have helped to establish the energy levels that are populated in the corresponding mercury daughter nuclides. Level schemes for Hg^{192}, Hg^{194}, Hg^{196}, and Hg^{198} deduced from the data are presented and discussed.

I. INTRODUCTION

THE modes of decay for both the high- and low-spin isomers of $Tl^{192,194,196,198}$ have been investigated in order to study the energy levels in the even-even daughter nuclei $Hg^{192,194,196,198}$. The thallium nuclides lie to the neutron-deficient side of the valley of β stability and can be reached only by high-energy proton-spallation reactions or by heavy-ion reactions. The desirability of studying nuclides lying away from the β-stability region has been discussed in recent articles by Bés[1] and by Bergström.[2] In addition, Bergström[3] has reviewed the experimental techniques available for such studies, especially the application of isotope separators.

The present work is part of a program to study neutron-deficient spallation products obtained from the bombardment of heavy targets with 3-GeV protons from the Princeton-Pennsylvania Accelerator (PPA). When a target of mass number A is irradiated with 3-GeV protons, the spallation products may have mass numbers from 1 to $A+1$. The Princeton electromagnetic isotope separator has been utilized to pick out of this complex mixture the particular isotope of interest. Isotopically pure samples with sufficient intensity for β-

† Work supported by the U. S. Atomic Energy Commission.
* Present address: Department of Physics, University of Oklahoma, Norman, Okla.
‡ Presently on leave at the Niels Bohr Institute, Copenhagen, Denmark.
§ Present address: Department of Chemistry, Lawrence University, Appleton, Wisc.

[1] D. R. Bés, Nucl. Instr. Methods **38**, 277 (1965).
[2] I. Bergström, Nucl. Instr. Methods **43**, 116 (1966).
[3] I. Bergström, Nucl. Instr. Methods **43**, 129 (1966).